# Square wave voltammetry measurements of low concentrations of nitrate using Au/AgNPs electrode in chloride solutions

Dancheng Chen Legrand, Carole Barus, Veronique Garcon

# Square wave voltammetry measurements of low concentrations of nitrate using Au/AgNPs electrode in chloride solutions

D. Chen Legrand[1], C. Barus[1*], V. Garçon

Laboratoire d'Etudes en Géophysique et Océanographie Spatiales, UMR 5566, Université de Toulouse, CNRS, CNES, IRD, UPS, 18 Avenue Edouard Belin 31401 TOULOUSE Cedex 9, France

[1] First co-authors
*Corresponding author
E-mail: carole.barus@legos.obs-mip.fr
Tel: +33 5 61 33 29 13
Fax: +33 5 61 25 32 05

## Abstract

The aim of this work is to highlight the potential of using a modified gold electrode with controlled quantity of silver nanoparticles as a working electrode to detect low concentrations of nitrate in chloride solutions. Optimal charge for silver deposition has been determined to obtain the highest signal for the nitrate reduction as the electrocatalytic properties of the bimetallic electrode were directly influenced by its composition. According to the Volcano plot obtained the charge chosen was -52 µC for a 3 mm diameter electrode, corresponding to 4.6 x $10^{15}$ Ag atoms $cm^{-2}$. It has been shown that dioxygen did not participate to the nitrate reduction mechanism. In order to decrease the limit of quantification, square wave voltammetry was preferred to less sensitive cyclic voltammetry. Nitrate was quantified in chloride solutions in the concentration range found in the open ocean, i.e. 0.39-50 µmol $L^{-1}$ with a good linear regression ($R^2$=0.9969). The stability of the bimetallic Au-Ag systems has been evaluated and showed almost no difference on the signal recorded over a 26 days period which is suitable to consider an *in situ* sensor development for marine applications.

## Keywords

Nanoparticles,

Electrocatalytic,

Nitration detection,

Square Wave Voltammetry,

Environmental chemistry.

# 1 - Introduction

The nitrogen cycle is one of the most important biogeochemical cycles in the marine environment. Nitrogen is found in five oxidation states: $^{(-III)}NH_4^+/NH_3$, $^{(0)}N_2$, $^{(+I)}N_2O$, $^{(+III)}NO_2^-$ and $^{(+V)}NO_3^-$ where $N_2$ is the most abundant species but essentially unreactive. Nitrate ($NO_3^-$) is the main form assimilated by marine organisms and as the other nutrients (silicate and phosphate) it can be used as a water mass tracer [1]. The concentration range found in the open ocean is from a few nanomolars to 50 µmol $L^{-1}$. Long term monitoring of nitrate ions concentration with *in situ* sensors is the key to improve our understanding of biogeochemical cycling in the ocean as well as to follow water masses and their mixing.

The classical technique to measure nitrate concentration in seawater is wet chemical colorimetry [2,3]. However, this method requires chemical reagents that need to be changed regularly and high power demand. Ultraviolet spectroscopy measurements at 220 nm are also used to detect nitrate ions in seawater [4]. *In situ* nitrate sensors for marine application using ultraviolet absorbance such as the ISUS (*In situ* Ultraviolet Spectrophotometer) or the SUNA (Submersible Ultraviolet Nitrate Sensor) are implementable on under-water vehicles such as ARGO profiling floats and they are already available on the market. However their sensitivity is still quite high, with a limit of detection around 1.5 µmol $L^{-1}$. In addition they suffer from strong chemical interferences such as with bromide ions, carbonates, or Colored Dissolved Organic Matter (CDOM) [5,6].

In order to decrease the limit of quantification, the cost and the size of sensors, electrochemistry is proposed to measure nitrate concentration in seawater. Nitrate being an electroactive species, it can be detected directly with electrochemical methods (voltammetry, amperometry…), no reagent is needed, which will facilitate miniaturisation of the detection system suitable for *in situ* analyses [2,7,8]. The electroreduction of nitrate has been intensively studied on various electrodes (Pt, Pd, Ni, Pb, Zn, Fe, Cu, Ti, Au, Au(Hg), Ru, Rh, Ir, Bi, Sn, alloys of Cu, Sn…) and is known to be a complex process [9,10]. Depending on the experimental conditions such as electrolyte anions [11], pH of the solution [12], nitrate concentration [13,14] and the structure of the working electrode [15], the mechanism is different and leads to nitrite ($NO_2^-$), ammonia ($NH_4^+$), nitrogen ($N_2$) as bi-products ($HNO_2$, $NO^+$, $NH_2OH$, $N_2O$…) [14,16,17]. Electrochemical sensors have been already used to detect nitrate in fresh water [18]. Hafezi and Majidi developed an amperometric sensor to detect nitrate in foodstuffs and mineral waters in the concentration range between 1 and 35 µmol $L^{-1}$ with a limit of detection of 0.59 µmol $L^{-1}$. However amperometry requires to stir the solution to control the convection which is not suitable for *in situ* sensor in seawater [19].

Among the electrodes, bimetallic electrodes showed a better sensitivity towards the detection of nitrate as the signal is enhanced due to higher specific electrode surface area [20-22]. The choice of electrode materials as well as the experimental conditions for

nanoparticles deposition to form the bimetallic electrodes are crucial and will have a large influence on the nitrate detection [23]. Previous work on gold modified with silver nanoparticles showed a good potential to detect nitrate in seawater [24]. However, the limit of quantification was still too high (i.e. 10 µmol $L^{-1}$) to consider *in situ* application in marine environments [24]. The aim of this work is to focus on the detection of low concentrations of nitrate in chloride solutions. To do so, an optimisation of the parameters to deposit silver nanoparticles on gold electrode is essential. Square wave voltammetry measurements are proposed to go further in terms of the sensitivity of our analytical method. To develop an *in situ* electrochemical sensor competitive with those already existing in oceanography, the limit of detection has to be the smallest possible (< 1.5 µmol $L^{-1}$[5]) and the modified electrode has to show a good stability with time.

## 2 - Experimental section

### 2.1 - Chemicals

All solutions were prepared in Milli-Q water (Millipore Milli-Q water system). Standard nitrate solutions were prepared with potassium nitrate ($KNO_3$, PURATRONIC®, 99.995 % purity) from Alfa Aesar in sodium chloride solution (NaCl, EMSURE®, supplied by Merck) at 34.5 g $L^{-1}$ (0.6 mol $L^{-1}$).

Sulphuric acid solution at 0.5 mol $L^{-1}$ used to clean electrode surfaces was prepared from a 98% $H_2SO_4$, EMSURE®, solution supplied by Merck.

Silver nanoparticles electrodepositions on gold electrode surfaces were made with silver nitrate $AgNO_3$ (AnalaR, NORMAPUR®, VWR Chemicals) dissolved in $KNO_3$ (Alfa Aesar) electrolyte solution.

### 2.2 - Material and methods

Chronoamperometry (I = f(t), fixed E), Cyclic Voltammetry (CV) (I = f(E)) and Square Wave Voltammetry (SWV) ($\triangle I = f(E_{step})$, with $\triangle I = I_{pulse\ forward} - I_{pulse\ backward}$) were performed in sodium chloride solutions ([NaCl] = 34.5 g $L^{-1}$) using a PGSTAT 128N potentiostat (Metrohm) controlled by NOVA software at room temperature under atmospheric conditions. A classical three electrodes system was used for all experiments. The counter electrode is a platinum grid purchased at GoodFellow. The reference electrode was a double junction Ag/AgCl/KCl (3 mol $L^{-1}$) electrode; all the potentials were referred to this electrode. The gold working electrode was a commercial gold disc electrode (ϕ = 3 mm) from Metrohm.

### 2.3 - Preparation of modified electrode Au/AgNPs

The gold disc surface was polished firstly with alumina (0.3 µm slurry diameter). Secondly, it was electrochemically cleaned in sulphuric acid solution ($H_2SO_4$, 0.5 mol $L^{-1}$) by polarising the electrode 10 seconds at +2 V and 10 seconds at -2 V to form $O_2$ and $H_2$ bubbles, respectively, at the electrode surface. Then, cyclic voltammograms were recorded between $E_1$ = 0 V and $E_2$ = 1.5 V at 100 mV $s^{-1}$ until reproducible cycles were obtained.

The electrodepositions of silver nanoparticles onto gold substrates were performed by chronoamperometry at E = -0.2 V optimised potential in a 0.1 mol $L^{-1}$ $KNO_3$ solution containing silver nitrate at [$AgNO_3$] = 0.17 mmol $L^{-1}$. The end of electrolyses was either controlled by the time of electrolysis (in seconds) or the electric charge (Q in Coulombs (C)). Several charges were studied in order to determine the optimised silver deposition. The resulting Au/AgNPs modified electrodes were then rinsed with MilliQ water. Cyclic voltammograms recorded with Au/AgNPs modified electrode in seawater highlighted the presence of silver on gold in the oxidation domain at +0.6 V (results not shown).

## 3 - Results and discussion

Fig. 1 shows cyclic voltammograms recorded on a gold commercial electrode (Au, Metrohm, ϕ = 3 mm) modified with silver nanoparticles (AgNPs) deposited at E = -0.2 V during 7 seconds, in sodium chloride solution (34.5 g $L^{-1}$) containing nitrate ions ([$NO_3^-$] = 9 mmol $L^{-1}$) at 20 and 500 mV $s^{-1}$ scan rates [24].

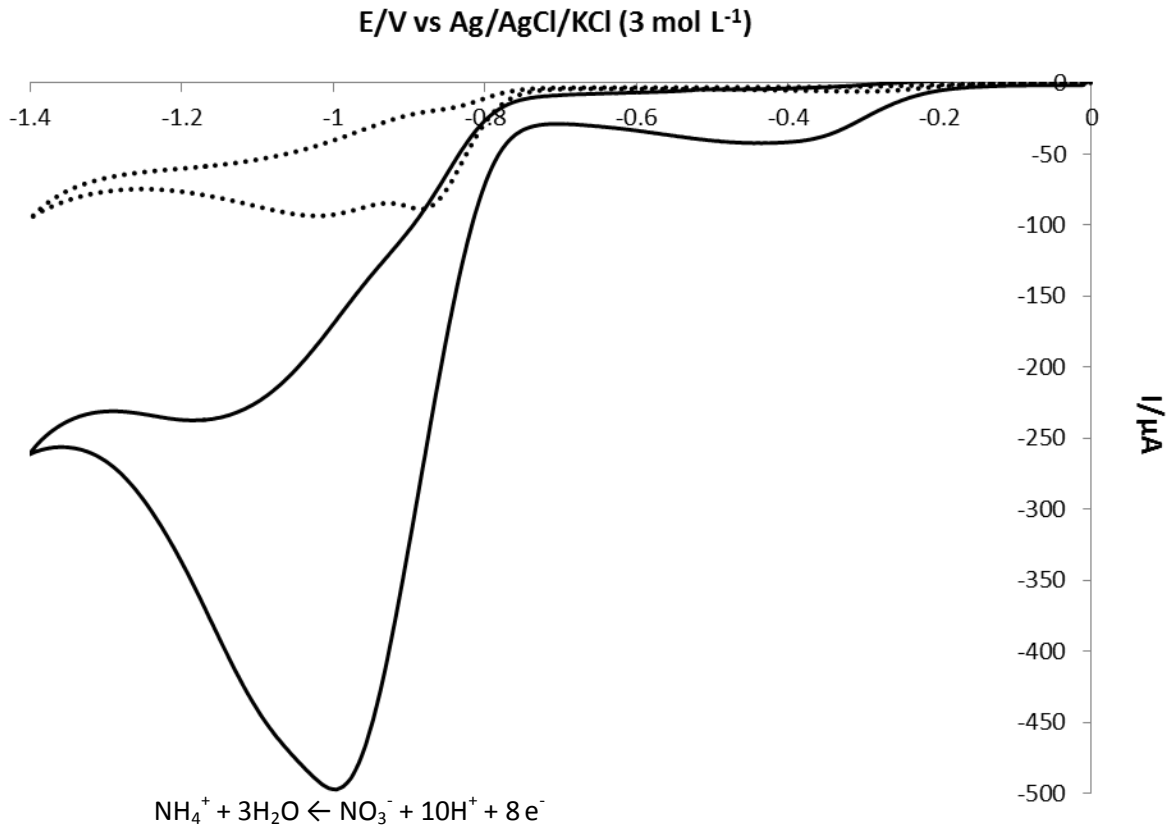


*Fig. 1*

The reduction starting around -0.2 V corresponds to the reduction of dioxygen. The reduction of nitrate occurs between -0.8 V and -1 V on Au/AgNPs surface. Only one peak is observed at -1.0 V at high scan rate (500 mV $s^{-1}$) whereas two peaks are visible around -0.9 V and -1.0 V, respectively, at lower scan rate (20 mV $s^{-1}$) showing the complexity of the mechanism. Aouina *et al.* also observed several reductions processes for nitrate reduction at 20 mV $s^{-1}$. They identified the formation of nitrite at the less negative potential and ammonia at the most negative potential [12]. Other authors also managed to highlight the formation of co-products depending on the experimental conditions (pH, electrolyte, nitrate concentration) used [10,12-17]. According to the bibliography, nitrate reduction requires first the adsorption of $NO_3^-$ on the electrode surface (reaction 1) [19,25,26]. The step determining the rate of the reaction on most electrodes is the reduction of $NO_{3\,(ads)}^-$ to $NO_{2\,(ads)}^-$ (reaction 2) [10]. The main final product is ammonia (reaction 3) [12,16,27].

$$NO_{3\,(sol)}^- \leftrightarrow NO_{3\,(ads)}^- \quad (1)$$

$$NO_{3\,(ads)}^- + 2H^+ + 2e^- \leftrightarrow NO_{2(ads)}^- + H_2O \quad (2)$$

$$NO_{2\,(ads)}^- + 8H^+ + 6e^- \leftrightarrow NH_4^+ + 2H_2O \quad (3)$$

The scan rate of v= 500 mV $s^{-1}$ is chosen to detect nitrate as the signal is much higher ($Ip_{(v=500\ mV\ s^{-1})}$ = 5.8 $Ip_{(v=20\ mV\ s^{-1})}$) than for the lower scan rate. It is also more convenient to treat only one, well defined, reduction peak than two tangled reduction waves.

As it was mentioned earlier, the structure of the bimetallic electrode has a strong influence on the signal [28]. Therefore, in order to improve the electrocatalytic properties of the electrode it is crucial to determine the optimum conditions for silver deposition on the gold working electrode.

In order to control the exact quantity of silver nanoparticles deposited on the gold surface (Metrohm, ϕ = 3 mm), the electrolyses at fixed potential (i.e. E = -0.2 V) realised to form Au/AgNPs electrodes are controlled by the charge in Coulomb (C) and not by the time. Depending on the initial state of the bare gold electrode, electrolyses controlled with time will give different Au/AgNPs electrodes as the AgNPs quantities deposited (charges) are not necessary the same from one electrolysis to another. The cut-off with the electric charge is the only way to ensure the deposition of the same quantity of silver nanoparticles.

The influence of charges (between -14 and -75 µC) used for silver deposition is investigated by analysing the cyclic voltammograms recorded with these different Au/AgNPs in sodium chloride solution (34.5 g $L^{-1}$) with 0.1 mmol $L^{-1}$ of nitrate. The forward cycles obtained for each charge are presented on Fig. 2.

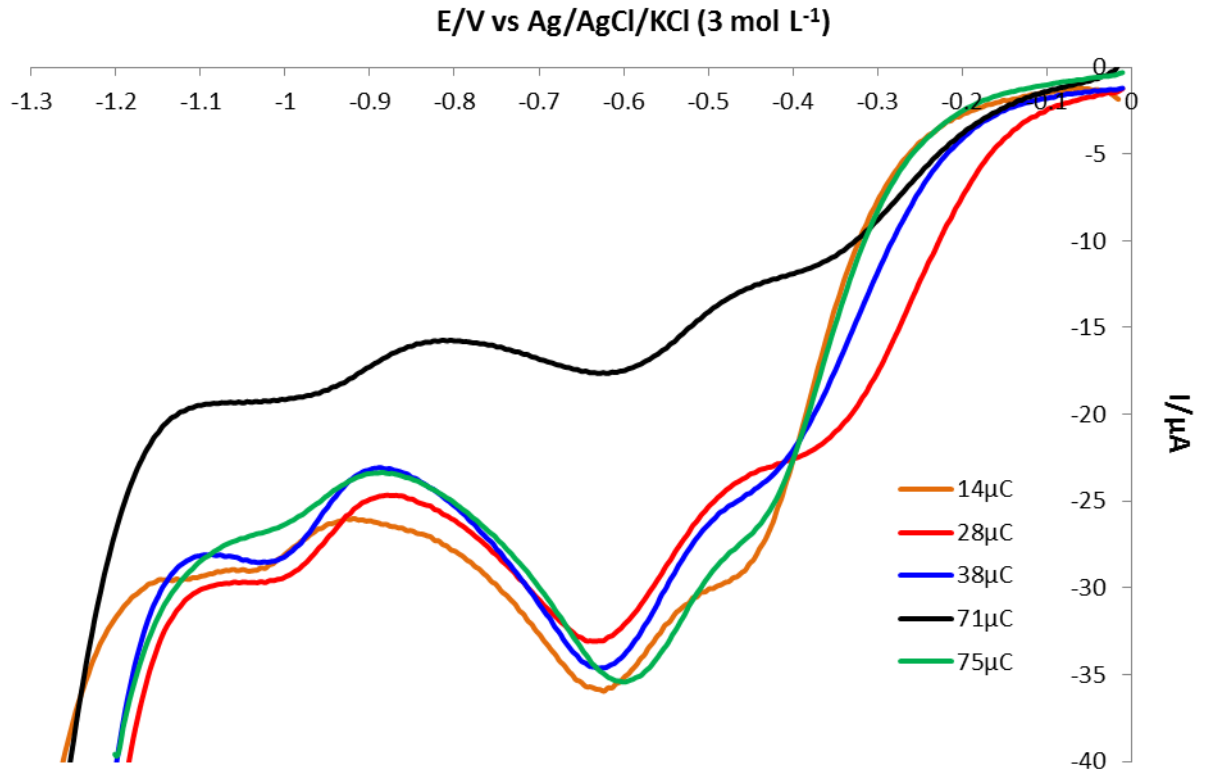

*Fig. 2*

The reduction of dioxygen appears on Fig. 2 in two peaks at -0.4 V and -0.6 V corresponding to the reduction of $O_2$ in two steps first into $H_2O_2$ then $H_2O$ observed on the gold electrode. For all the charges applied, the gold electrodes are therefore not totally covered with silver. Even if the experiments were realised in atmospheric conditions, with saturated $O_2$ solutions, the signal observed on Fig. 2 for $O_2$ varies from one experiment to the other and might have an influence on $NO_3^-$ measurements. The influence of $O_2$ on nitrate measurement will be checked later on.

As expected the intensity corresponding to nitrate reduction increases when the silver electrodeposition charge increases from -14 µC to -38 µC as the effective surface area of the electrode increased (Fig. 2). However, increasing too much the charge leads to a decrease of nitrate signal for -71 µC and -75 µC (Fig. 2). This result is more visible on the corresponding Volcano plot ($I_{peak}$=f(|Q|)) presented on Fig. 3 showing two characteristic linear slopes. This behaviour has been observed in the bibliography and can be explained by the Ostwald ripening widely known in the field of crystallization and corresponding to the dissolution of smaller particles that will grow in larger ones [29-31]. The effective surface area of Au/AgNPs therefore decreases and the electrode tends to behave as a bare electrode. The mechanism of Ostwald ripening includes a diffusion process at the surface and grain boundary, and an electrochemical mechanism. Larger and smaller particles behave as different metals with different standard electrode potentials explaining that it is easier to reduce $NO_3^-$ on electrode with smaller particles than on a bulk material or on larger particles electrode [30]. Adsorption is also promoted on small nanoparticles as the effective surface is bigger and so makes the reduction on this electrode easier. This is why pure bare gold electrode is inactive toward nitrate reduction (weak adsorption of the reactants) [26]. The maximum catalytic activity should be for a surface partially covered with AgNPs which is the case for all the charges tested as the characteristic reduction of $O_2$ in two steps on gold is always visible on Fig. 2. Therefore, in order to obtain the highest $NO_3^-$ signal the charge to deposit AgNPs has to be the highest possible but before the Ostwald ripening process starts. According to the Sabatier principle, the best condition is determined on Volcano plot (Fig. 3), corresponding to the intersection of the 2 straight lines ($I_{peak}$ = f (|Q|)) [26,32]. The optimum charge found to form the modified Au/AgNPs electrode and to detect $NO_3^-$ is -56.3 µC. Taking into account the experimental errors to build the Volcano plot and determine the optimum condition, the charge chosen for silver nanoparticles deposition is -52 µC corresponding to 4.6 x $10^{15}$ Ag atoms $cm^{-2}$.

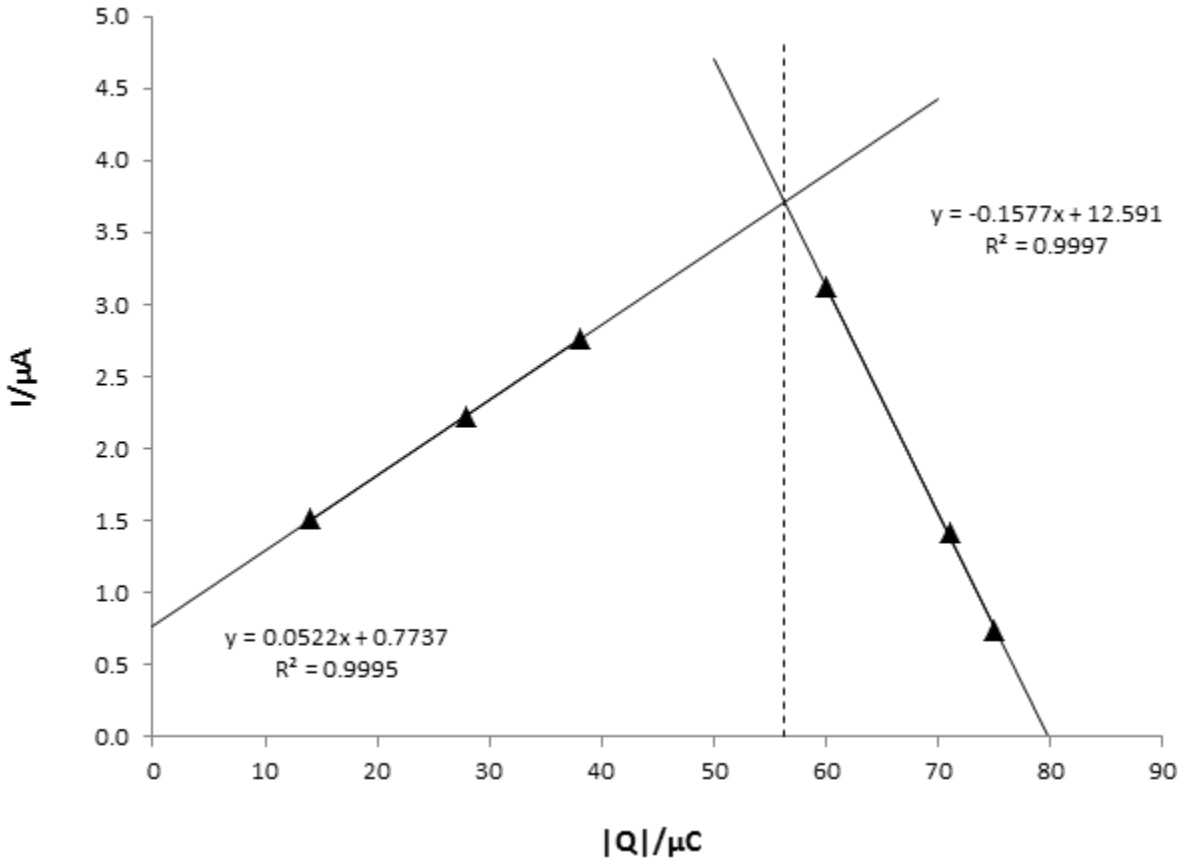


*Fig. 3*

In the open ocean, the concentrations of dissolved dioxygen vary from 300 µmol $L^{-1}$ in saturated surface waters down to around 50 µmol $L^{-1}$ for deeper waters. Some areas called Oxygen Minimum Zones (OMZ) are very depleted in dioxygen in sub-surface where the concentration can be close to zero [33]. On the potential window used, the dioxygen reduces just before the potential of nitrate reduction and variations of its signal have been observed even in oxygenated solutions (Fig. 2). It might have an influence on nitrate reduction even more if its concentration changes from an experiment to another. Therefore in order to study the influence of dioxygen reduction on the nitrate detection, cyclic voltammograms were recorded with the same modified electrode (Au/AgNPs: Q = -68 µC) on the same nitrate solution at 1 mmol $L^{-1}$ with and without dioxygen. The solution has been deaerated during 15 minutes with nitrogen bubbling to remove all the dioxygen and a constant flow of nitrogen was maintained over the surface during the experiment to prevent dioxygen to diffuse into the solution. The results are presented on Fig. 4.

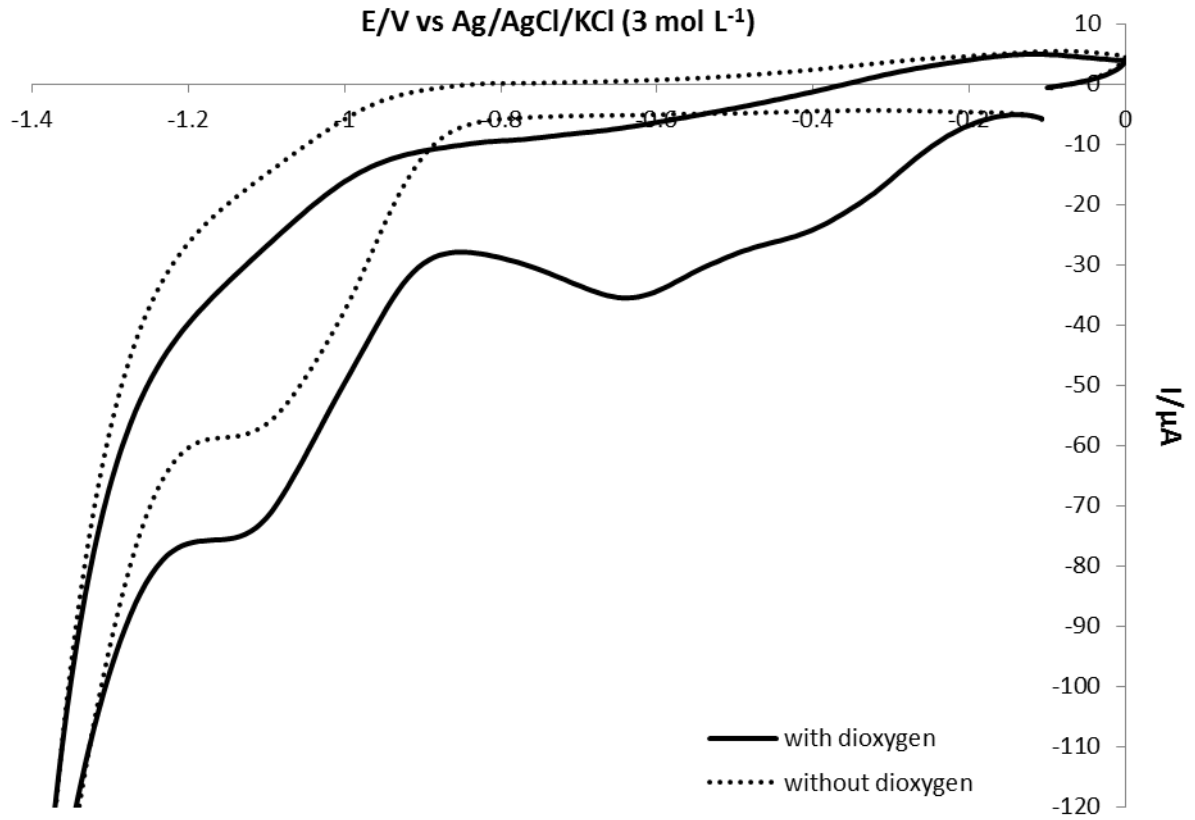


*Fig. 4*

Fig. 4 shows indeed the disappearance of the two dioxygen peaks at -0.4 V and -0.6 V after 15 minutes of nitrogen bubbling. But in both cases, the peak intensities at E = -1.1 V corresponding to nitrate reduction are identical (~50 µA). Almost the same result has been obtained by Gross *et a*l. in 2015 on Au/AgNPs electrode where the difference observed on the signals with and without dioxygen was extremely weak (experimental errors) [34]. The $O_2$ has therefore no influence on nitrate detection using Au/AgNPs electrode unlike previous work by Fajerwerg *et al.* suggested [24]. They proposed a catalytic reaction between the intermediate oxygen peroxide formed from the incomplete reduction of dioxygen on gold electrode with nitrite ions produced from the incomplete nitrate reduction. However, the increase of $NO_3^-$ peak intensity they observed on Au/AgNPs is probably due to an increase of electroactive surface area of the modified electrode Au/AgNPs from one deposition to the other as the amount of silver nanoparticles deposited was not controlled with the electric charge but with the time of electrolysis. In conclusion, the mechanism of nitrate reduction however complicated it may be, is clearly not influenced by dioxygen which is compatible with our aim to develop a new electrochemical sensor in the open ocean where $O_2$ concentration varies significantly throughout the water column.

Now in order to go further on the detection of low concentrations of nitrate using the optimized Au/AgNPs (Q = -52 µC) electrode, square wave voltammetry method is proposed to detect nitrate. This electrochemical method is more sensitive than cyclic voltammetry thanks to short-term square shape potential pulses combined with staircase potential ramp and current sampling allowing to decrease the contribution of capacitive current. This pulse technique is attractive for quantitative analysis since it leads to better resolved peaks (Gaussian shape), less distorted by the capacitive current. Indeed, in order to obtain the highest sensitivity (corresponding to the electron(s) transfer), it is important to reduce the effect of the capacitive current and only measure the contribution of the faradic current. The current is therefore sampled at the end of each potential pulse (forward pulse and backward pulse) as the faradaic current ($I_f \propto t^{-1/2}$) decreases slower than the capacitive current ($I_c \propto e^{-t/RC}$) with time [35].

The SWV parameters have been optimized to obtain the least noisy signal possible using classical frequency of *f* = 100 Hz, an amplitude of $E_{SW}$ = 60 mV and a staircase potential $E_{step}$ = 5 mV, corresponding to the same scan rate than previously used with cyclic voltammetry (i.e. 500 mV $s^{-1}$). Common values for amplitude and step potential are respectively $E_{SW} = \frac{50}{n}$ and $E_{step} = \frac{10}{n}$, with n the number of electron(s) exchanged [36]. So considering the reduction of $NO_3^-$ into $NO_2^-$, 2 electrons are exchanged and $E_{SW}$ should be around 25 mV and $E_{step}$ around 5 mV. However experimental results showed better resolution with higher amplitude. Indeed, amplitude affects the electrode kinetics of the electrode reaction. Higher amplitude gives higher net response in current, however too large amplitude may lead to interferences by the charging current and the ohmic drop resistance [37]. The result obtained for 100 mV amplitude (result not shown) was indeed not satisfying and much noisy, so 60 mV amplitude has been fully validated.

The square wave voltammograms obtained with Au/AgNPs (ϕ = 3 mm, Q = -52 µC) electrode for nitrate concentrations between 0.39 and 50 µmol $L^{-1}$ are presented on Fig. 5. As previously observed on cyclic voltammograms, three peaks are observed at -0.25, -0.6 and -1.0 V corresponding respectively to the reduction on gold surface in two steps of $O_2$ into $H_2O_2$ then $H_2O_2$ into $H_2O$ and finally the reduction of $NO_3^-$ where the peak intensities increase with $NO_3^-$ concentrations. The fact that signals show positive current even for reduction processes is due to the amplitude chosen for the pulses as the differential intensities ($\triangle I = I_{forward} - I_{backward}$) are plotted versus staircase potential [38].

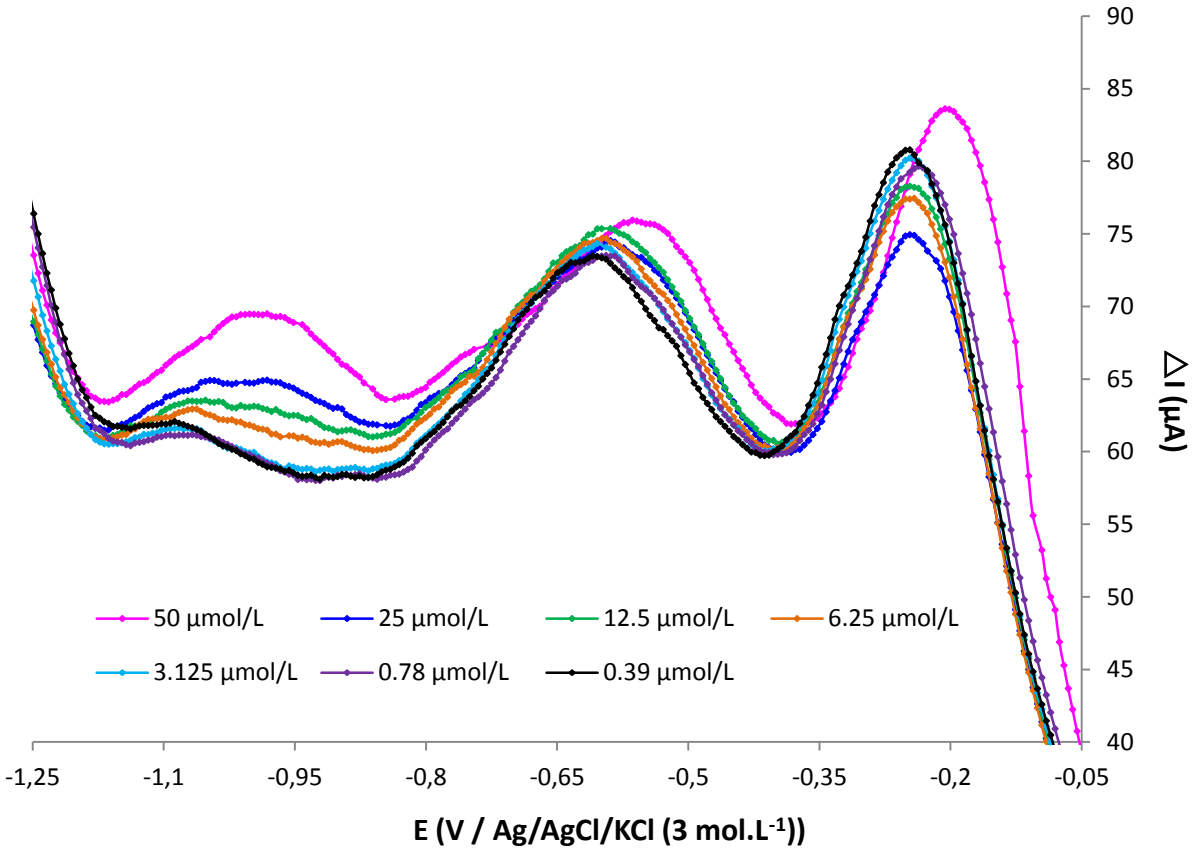


*Fig. 5*

A shift of nitrate peak potential towards more anodic potentials (from -1.1 V to -0.9 V) (less negative potentials) is observed on Fig. 5 when $NO_3^-$ concentration increases indicating an easier electronic transfer at high concentration than at low $NO_3^-$ concentration. This result has also been observed by Bui *et al.,* on different pulse voltammetry measurements on carbon paper electrode functionalised with gold nanoparticles [18].

As it has been mentioned before, the nitrate electroreduction mechanism is influenced by the nitrate concentration and requires as well the adsorption of nitrate on the electrode surface before its reduction [14,26]. Considering the adsorption reaction (1), the equilibrium of the reaction might shift towards the formation of $NO_3^-{}_{(ads)}$ if the $NO_3^-{}_{(sol)}$ increases, facilitating its reduction, therefore explaining the anodic peak potential shifting observed. Also the nitrate adsorption is quite weak and strongly influenced by the adsorption of anions and hydrogen (particularly on platinum electrodes) [13,15]. There is therefore a competition on the electrode surface between $NO_3^-{}_{(ads)}$ and adsorbed anions ($Cl^-$) making harder the adsorption of nitrate ions especially at really low concentrations.

The peak intensities for each concentration have been measured using NOVA software and the corresponding calibration curve is presented on Fig. 6. A good linear behaviour is obtained between 0.39 µmol $L^{-1}$ up to 50 µmol $L^{-1}$ which covers the whole concentration range found in the open ocean. The limit of quantification is 0.39 µmol $L^{-1}$.

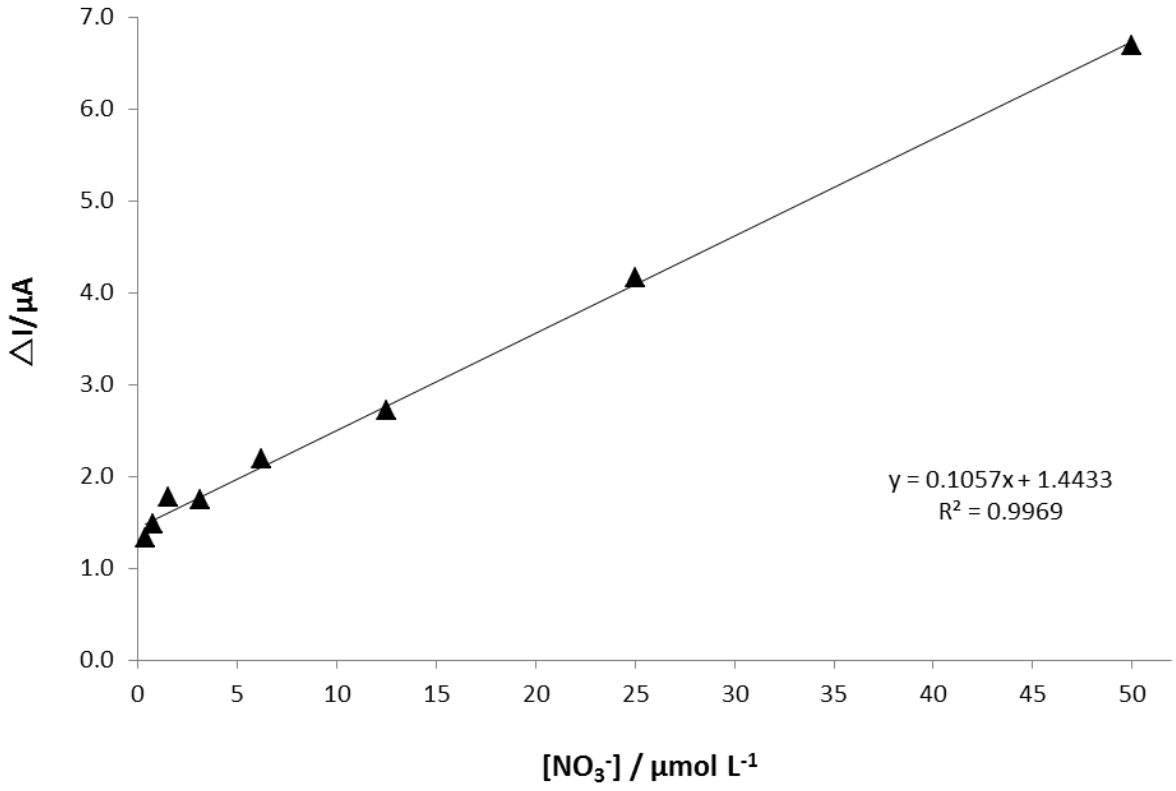


*Fig. 6*

Now, in order to use this modified electrode in a sensor for marine applications, its stability with time has to be evaluated particularly the stability of the silver nanoparticles.
The same modified electrode Au/AgNPs (ϕ = 3mm, Q = -52 µC) is continuously stored in sodium chloride solution and used to detect regularly nitrate at $[NO_3^-]$ = 25 µmol $L^{-1}$ using square wave voltammetry during 625 hours (~26 days). The peak intensity corresponding to nitrate reduction remained at 95 % from the initial intensity peak (t=0) for 26 days showing quite a good stability of the system and its potential as an electrode in a marine sensor.

## 4 - Conclusions

The results presented in this work show a sensitive method for the nitrate detection in sea water using a very simple three electrodes electrochemical system. The study of the influence of the electric charge to deposit silver particles on nitrate detection allowed to determine the best conditions to enhance the electrocatalytic properties of the bimetallic electrode. The optimum charge found is Q = -52 µC corresponding to ~4.6 x $10^{15}$ Ag atoms $cm^{-2}$. A very good calibration has been obtained using this modified Au/AgNPs electrode and square wave voltammetry measurements on the concentration range found in the open ocean (0.39 – 50 µmol $L^{-1}$) with a limit of quantification of 0.39 µmol $L^{-1}$. Finally the study of the electrode stability in time showed a good potential for *in situ* use.

To decrease the LOD of nitrate detection, a larger electrode surface could be used in order to increase the intensity. Also a comparison with other bimetallic couples should be tried as copper showed very good electrocatalytic properties for nitrate detection [19] or platinum substrate instead of gold for example.

## Acknowledgments

The present work was supported by the MIACTIS project: “Microsystèmes intégrés pour l’analyse des composés en traces *in situ*” (Integrated microsystems for the analyses of *in situ* trace compounds) as part of the overall project “Instrumentation and Environmental Sensors” funded by the RTRA-STAE: thematic network of the foundation for scientific cooperation “Sciences et Technologies pour l’Aéronautique et l’Espace” (Sciences and Technologies for Aeronautic and Space) in Toulouse, France.

## References


[1] B.B. Ward, D.G. Capone, J.P. Zehr, Oceanography 2007, **20**, 101-109.

[2] M.J. Moorcroft, J. Davis, R.G. Compton, Talanta 2001, **54**, 785-803.

[3] M.D. Patey, M.J.A. Rijkenberg, P.J. Statham, M.C. Stinchcombe, E.P. Achterberg, M. Mowlem, Trends Anal. Chem. 2008, **27**, 169-182.

[4] M.S. Finch, D.J. Hydes, C.H. Clayson, B.Weigl, J.Dakin, P.Gwilliam, Anal. Chim. Acta 1998, **377**, 167-177.

[5] K.S. Johnson and L.J. Coletti, Deep Sea Res., Part I 2002, **49**, 1291-1305.

[6] K.S. Johnson, L.J. Coletti, H.W. Jannasch, C.M. Sakamoto, D.D. Swift and S.C. Riser, J. of Atmos. Oceanic Technol. 2013, **30**, 1854-1866.

[7] N.G. Carpenter and D. Pletcher, Anal. Chim. Acta 1995, **317**, 287-293.

[8] A.S. Koparal and U.B. Ogutveren, J. Hazard. Mater. 2002, **89**, 83-94.

[9] Inam-Ul-Haque and M. Tariq, J. Chem. Soc. Pak. 2010, **32**, 396-418.

[10] G.E. Dima, A.C.A de Vooys, M.T.M. Koper, J. Electroanal. Chem. 2003, **554-555**, 15-23.

[11] D. Pletcher and Z. Poorabedi, Electrochim. Acta 1979, **24**, 1253-1256.

[12] N. Aouina, H. Cachet, C. Debiemme-Chouvy, T.T. Mai Tran, Electrochim. Acta 2010, **55**, 7341-7345.

[13] V. Rosca, M. Duca, M.T. de Groot and M. T. M. Koper, Chem. Rev. 2009, **109**, 2209-2244.

[14] M.T. de Groot and M.T.M. Koper, J. Electroanal. Chem. 2004, **562**, 81-94.

[15] G.E. Dima, G.L. Beltramo, M.T.M. Koper, Electrochim. Acta 2005, **50**, 4318-4326.

[16] F.M. Cuibus, A. Ispas, A. Bund, P. Ilea, J. Electroanal. Chem. 2012, **675**, 32-40.

[17] R. Lange, E. Maisonhaute, R. Robin, V. Vivier, Electrochem. Commun. 2013, **29**, 25-28.

[18] M.-P. N. Bui, J. Brockgreitens, S. Ahmed, A. Abbas, Biosens. Bioelectron. 2016, **85**, 280-286.

[19] B. Hafezi and M.R. Majidi, Anal. Methods 2013, **5**, 3552-3556.

[20] M.J. Moorcroft, J. Davis, R.G. Compton, Talanta 2001, **54**, 785-803.

[21] J. Davis, M.J. Moorcroft, S.J. Wilkins, R.G. Compton, M.F. Cardosi, Analyst 2000, **125**, 737-742.

[22] U. Prüsse and K.-D. Vorlop, J. Mol. Catal. A: Chem. 2001, **173**, 313-328.

[23] J. Liang, Y. Zheng, Z. Liu, Sens. Actuators, B 2016, **232**, 336-344.

[24] K. Fajerwerg, V. Ynam, B. Chaudret, V. Garçon, D. Thouron, M. Comtat, Electrochem. Commun. 2010, **12**, 1439-1441.

[25] A. Pintar, J. Batista, J. Levec, T. Kajiuchi, Appl. Catal., B 1996, **11**, 81-98.

[26] F. Calle-Vallejo, M. Huagn, J.B. Henry, M.T.M. Koper, A.S. Bandarenka, Phys. Chem. Chem. Phys. 2013, **15**, 3196-3202.

[27] J. Christophe, V. Tsakova, C. Buess-Herman, Z. Phys. Chem. 2007, **221**, 1123-1136.

[28] M.R. Majidi, K. Asadpour-Zeynali, B. Hafezi, Int. J. Electrochem. Sci. 2011, **6**, 162-170.

[29] N. Serizawa, Y. Katayama, T. Miura, Electrochim. Acta 2010, **56**, 346-351.

[30] P.L. Redmond, A.J. Hallock, L.E. Brus, Nano Lett. 2005, **5**, 131-135.

[31] F. Wang, R. Han, G. Liu, H. Chen, T. Ren, H. Yang, Y. Wen, J. Electroanal. Chem. 2013, **706**, 102-107.

[32] A.B. Laursen, A.S. Varela, F. Dionigi, H. Fanchiu, C. Miller, O.L. Trinhammer, J. Rossmeils, S. Dahl, J. Chem. Educ. 2012, **89**, 1595-1599.

[33] A. Paulmier and D. Ruiz-Pino, Prog. Oceanogr. 209, **80**, 113-128.

[34] A.J. Gross, S. Holmes, S.E.C Dale, M.J. Smallwood, S. J. Green, C.P. Winlove, N. Benjamin, P.G. Winyard, F. Marken, Talanta 2015, **131**, 228-235.

[35] V. Mirčeski, Š. Komorsky-Lovrić, M. Lovrić, *Square-Wave Voltammetry : Theory and Application* ; Editor F. Scholz, Springer, **2007**.

[36] A. Bard and L.R. Faulkner, *Electrochemical Methods: Fundamentals and Applications* Chapter 7, 2nd ed., John Wiley and Sons, **2001**.

[37] V. Mirceski, E. Laborda, D. Guziejewski, R. G. Compton ; Anal. Chem. 2013, **85**, 5586-5594.

[38] M. Lovric and D. Jadresko, Electrochim. Acta 2010, **55**, 948-951.

## Figure captions

Fig. 1: Influence of the scan rate on the cyclic voltammograms obtained in NaCl solution (34.5 g $L^{-1}$) containing 9 mmol $L^{-1}$ $KNO_3$ using Au/AgNPs (E = -0.2 V, t = 7 s) at scan rate 20 mV $s^{-1}$(·····) and 500 mV $s^{-1}$ (—)

Fig. 2: Influence of charge used for Ag deposition on forward cycles of cyclic voltammograms obtained in NaCl solution (34.5 g $L^{-1}$) containing 0.1 mmol $L^{-1}$ $KNO_3$ using Au/AgNPs electrodes - Q = -14 µC (Orange), Q= -28 µC (Red), Q = -38 µC (Blue), Q = -71 µC (Black) and Q= -75 µC (Green); scan rate: 500 mV $s^{-1}$

Fig. 3: Volcano plot $I_{peak}(NO_3^-) = f(|Q|)$ corresponding to the Fig. 2

Fig. 4: Influence of dioxygen on cyclic voltammograms obtained in NaCl solution (34.5 g $L^{-1}$) containing 1 mmol $L^{-1}$ $KNO_3$ using Au/AgNPs electrode (Q = -68 µC) with dioxygen (straight line) and without dioxygen (dotted line); scan rate: 500 mV $s^{-1}$

Fig. 5: Square wave voltammograms at f = 100 Hz, $E_{SW}$ = 60 mV, $E_{step}$ = 5 mV on Au/AgNPs (ϕ = 3 mm / Q = -52 µC) in 34.5 g $L^{-1}$ NaCl solution containing $[NO_3^-]$ = 0.39 (black), 0.78 (purple), 3.125 (light blue), 6.25 (orange), 12.5 (green), 25 (dark blue) and 50 µmol $L^{-1}$ (pink)

Fig. 6: Calibration curve $\triangle I = f([NO_3^-])$ for peak around E = -1.0 V from SWV on Fig. 6 between 0.39 and 50 µmol $L^{-1}$